Individual differences in the neural strategies to control the lateral and medial head of the quadriceps during a mechanically constrained task

Simon Avrillon, Alessandro del Vecchio, Dario Farina, José Pons, Clément Vogel, Jun Umehara, François Hug

american physiological society

JOURNAL OF APPLIED PHYSIOLOGY

J Appl Physiol 130: 269–281, 2021.
First published November 26, 2020; doi:10.1152/japplphysiol.00653.2020

RESEARCH ARTICLE

Individual differences in the neural strategies to control the lateral and medial head of the quadriceps during a mechanically constrained task

Simon Avrillon,[1,2,3] Alessandro Del Vecchio,[4,5] Dario Farina,[5] José L. Pons,[1,2] Clément Vogel,[3] Jun Umehara,[6,7] and François Hug[3,8,9]

[1]*Legs + Walking AbilityLab, Shirley Ryan AbilityLab, Chicago, Illinois;* [2]*Department of Physical Medicine and Rehabilitation, Northwestern University, Chicago, Illinois;* [3]*Laboratory Movement, Interactions, Performance, Université de Nantes, Nantes, France;* [4]*Department of Artificial Intelligence in Biomedical Engineering, Friedrich-Alexander University, Erlangen-Nürnberg, Erlangen, Germany;* [5]*Neuromechanics and Rehabilitation Technology Group, Department of Bioengineering, Faculty of Engineering, Imperial College, London, United Kingdom;* [6]*Department of Human Health Sciences, Graduate School of Medicine, Kyoto University, Kyoto, Japan;* [7]*Japan Society for the Promotion of Science, Tokyo, Japan;* [8]*School of Health and Rehabilitation Sciences, The University of Queensland, Brisbane, Australia; and* [9]*Institut Universitaire de France, Paris, France*

Abstract

The interindividual variability in the neural drive sent from the spinal cord to muscles is largely unknown, even during highly constrained motor tasks. Here, we investigated individual differences in the strength of neural drive received by the vastus lateralis (VL) and vastus medialis (VM) during an isometric task. We also assessed the proportion of common neural drive within and between these muscles. Twenty-two participants performed a series of submaximal isometric knee extensions at 25% of their peak torque. High-density surface electromyography recordings were decomposed into motor unit action potentials. Coherence analyses were applied on the motor unit spike trains to assess the degree of neural drive that was shared between motor neurons. Six participants were retested ~20 mo after the first session. The distribution of the strength of neural drive between VL and VM varied between participants and was correlated with the distribution of normalized interference electromyography (EMG) signals ($r > 0.56$). The level of within- and between-muscle coherence varied across individuals, with a significant positive correlation between these two outcomes (VL: $r = 0.48$; VM: $r = 0.58$). We also observed a large interindividual variability in the proportion of muscle-specific drive, that is, the drive unique to each muscle (VL range: 6%–83%, VM range: 6%–86%). All the outcome measures were robust across sessions, providing evidence that the individual differences did not depend solely on the variability of the measures. Together, these results demonstrate that the neural strategies to control the VL and VM muscles widely vary across individuals, even during a constrained task.

NEW & NOTEWORTHY We observed that the distribution of the strength of neural drive between the vastus lateralis and vastus medialis during a single-joint isometric task varied across participants. Also, we observed that the proportion of neural drive that was shared within and between these muscles also varied across participants. These results provide evidence that the neural strategies to control the vastus lateralis and vastus medialis muscles widely vary across individuals, even during a mechanically constrained task.

coherence; common drive; electromyography; motor units; quadriceps

INTRODUCTION

It is well known that different people can perform the same motor task with different motor coordination strategies, leading to the notion of individual movement signature (1, 2) or individuality (3). As movements result from the complex interplay between neural commands to the muscles and the properties of the neuromusculoskeletal system (4), identifying the mechanisms underlying these individual differences in movement patterns is challenging. For example, the role of the neural commands in these individual differences is largely unknown.

A number of studies report interindividual differences in electromyography (EMG) signals measured using surface electrodes during multijoint tasks (2, 5–8). Such differences are also observed during mechanically constrained tasks where fewer opportunities for individual variation are theoretically available. For example, large individual differences in the distribution of normalized EMG amplitude between the lateral head [vastus lateralis (VL)] and the medial head

Correspondence: F. Hug (francois.hug@univ-nantes.fr).
Submitted 5 August 2020 / Revised 6 November 2020 / Accepted 11 November 2020

[vastus medialis (VM)] of the quadriceps have been observed during a submaximal isometric knee extension (9, 10). Even though these individual differences are often interpreted as differences in neural strategies, this interpretation requires further consideration.

Most of the aforementioned studies used conventional bipolar surface EMG recordings. In addition to the issue of the poor selectivity of the surface EMG signals, surface EMG amplitude only provides a crude index of the neural drive that is sent to the muscles from the innervating motor neurons (11, 12). For example, Martinez-Valdes et al. (13) compared the strength of neural drive received by the VL and VM muscles during isometric contractions by comparing the increase in discharge rate of motor units matched by recruitment threshold. Despite the fact that they observed a greater normalized EMG amplitude for VL than VM, they estimated that these two muscles received a similar level of neural drive. Of note, this observation was performed at the group level (the data were averaged over the group of participants), and it remains unknown whether the distribution of neural drive between these synergist muscles varied across the participants.

In addition to the strength of neural drive received by individual muscles, understanding the control of muscle coordination requires knowledge of the proportion of shared and independent synaptic input received by the pools of motoneurons. To this end, correlations in the time and frequency domains are classically performed from interference EMG signals (14, 15). However, EMG cross talk substantially influences these estimates (16). At the individual motor unit level, Laine et al. (17) demonstrated that the VL and VM muscles share most of their synaptic input during an isometric knee extension. To our knowledge, no studies have focused on the interindividual variability in the level of common input shared within and between synergist muscles.

In this study, we characterized individual neural strategies to control the VL and VM muscles during a highly mechanically constrained task, that is, submaximal torque-matched isometric knee extension. We first aimed to determine the individual differences in the strength of neural drive received by the VL and VM and its relationship with interference EMG amplitude. Second, we aimed to determine the individual differences in the degree of common input within and between the motor neuron pools innervating each muscle. To address these aims, we recruited a homogeneous sample to exclude variability due to age, gender, or physical activity, as these factors can generate variability in neural control (18, 19). We used high-density surface electromyography (HDsEMG) to identify the behavior of motor units from the VL and VM muscles. We hypothesized that individuals would exhibit variations in the distribution of the strength of neural drive between VL and VM and that these variations will be related to those observed with interference EMG. Also, because the effective neural drive to muscles is determined by the common synaptic input to motor neurons (20), we hypothesized that there would be interindividual variations in the estimated common input within and between muscles. To rule out the possibility that the interindividual variations depended solely on variability of the measures, a subset of participants (n = 6) was retested ~20 mo after the first session to verify the robustness of the outcome measures.

METHODS

Participants

Twenty-two healthy men (age: 25 ± 5 yr; height: 178 ± 6 cm; body mass: 70 ± 7 kg) participated in this experiment. Of these 22 participants, six underwent a second experimental session 20 mo later (±1 month). Participants had no history of knee injury or lower leg pain that would limit function within the previous 6 mo. The ethics committee "Comité de protection des personnes Ile de France XI" approved the study (CPP-MIP-013), and all procedures adhered to the Declaration of Helsinki. Participants provided an informed written consent.

Protocol

Participants performed isometric knee extension tasks on a dynamometer (Biodex System 3 Pro, Biodex Medical, Shirley, NY). Participants sat on the dynamometer with their hip flexed at 90° (0° = neutral position) and their knee flexed at 80° (0° = full extension) (Fig. 1). Two inextensible straps were used to immobilize their torso.

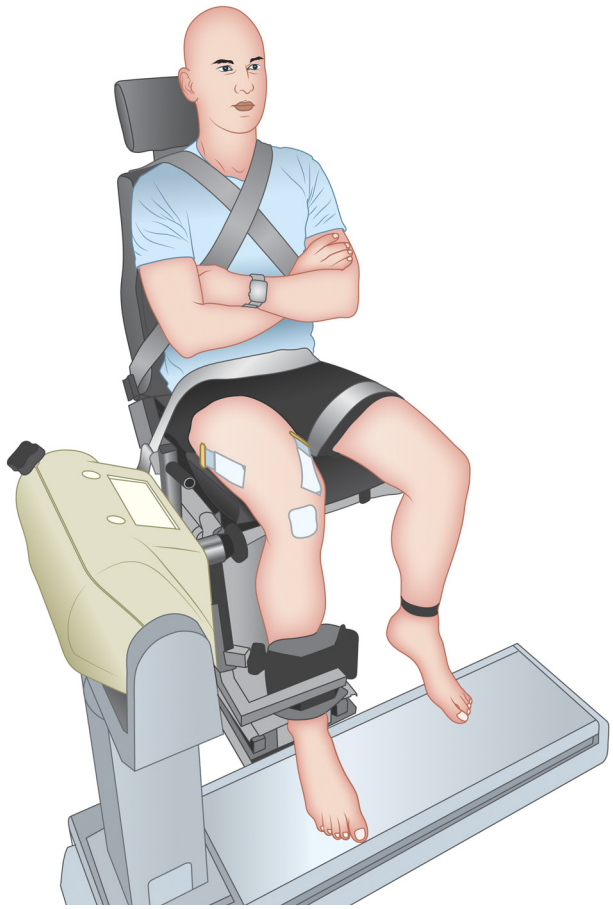

Figure 1. Experimental setup and placement of the high-density electromyography electrodes. A two-dimensional adhesive grid of 64 electrodes was placed over both the vastus lateralis (VL) and the vastus medialis (VL) muscle.

The experiment began with a standardized warm-up, which included a series of 20 isokinetic contractions at $60^{\circ}\cdot s^{-1}$ and four submaximal isometric contractions at 60%, 70%, 80%, and 90% of their subjective maximal isometric torque for 3–4 s, with 60 s of rest in between. Then, participants performed three maximal isometric contractions (MVCs) for 3–5 s, with 120 s of rest in between. The maximal value obtained from a moving average window of 250 ms was considered as the peak torque. Then, participants performed three torque-matched contractions at 25% of their peak torque. These contractions involved a 10-s ramp-up, a 10-s plateau, and a 10-s ramp-down phase. They were separated by 30 s of rest. Feedback from the target and torque output was displayed on a monitor. The torque signal was digitized at 2048 Hz using the same acquisition system that was used for HDsEMG (EMG-Quattrocento; 400-channel EMG amplifier, OT Bioelettronica, Italy).

High-Density Surface EMG Recording

HDsEMG signals were recorded from the VL and VM muscles. A two-dimensional adhesive grid of 64 electrodes [13 × 5 gold-coated electrodes with one electrode absent on a corner; interelectrode distance: 8 mm (ELSCH064NM2, OT Bioelettronica, Italy)] was placed over each muscle. The grids were aligned in the direction of the fascicles, which was determined using B-mode ultrasonography (Aixplorer, Supersonic Imagine, France). Specifically, the fascicle direction was considered as the main axis of the transducer when continuous fascicle(s) and clear muscle aponeurosis could be seen on the image. Before mounting the electrode grids, the skin was shaved and was then cleansed with an abrasive pad and alcohol. The adhesive grids were held on the skin using semidisposable biadhesive foam layers (SpesMedica, Battipaglia, Italy). The skin-electrode contact was made by filling the cavities of the adhesive layers with conductive paste (SpesMedica, Battipaglia, Italy). Reference electrodes (Kendall Medi-Trace, Canada) were placed over the patella. The EMG signals were recorded in monopolar mode, were bandpass filtered (10–500 Hz), and were digitized at a sampling rate of 2048 Hz using a multichannel HDsEMG acquisition system (EMG-Quattrocento, 400 channel EMG amplifier; OT Bioelettronica).

Data Analysis

Data were analyzed using MATLAB custom-written scripts (R2017a; The MathWorks, Natick, MA).

Force signals.

Torque signals were low-pass filtered (third-order Butterworth filter, cutoff frequency: 20 Hz). We calculated the coefficient of variation of the torque over the plateau as an estimation of task performance, that is, the lower the coefficient of variation, the higher the ability of the participant to track the target.

Global EMG.

To estimate the normalized EMG amplitude with the HDsEMG electrodes, single differential signals were first calculated as the differences between adjacent electrodes in the column direction. This resulted in 59 differential signals. Each EMG signal was visually inspected for noise and artifacts. Signals that exhibited noise or artifacts were excluded and replaced by the linear interpolation of all the adjacent channels (between two and four depending on the location of the electrode). During MVC, the average rectified value (ARV) was calculated for each of the 59 signals over a moving time window of 250 ms. For each channel, the maximal ARV achieved over the three contractions was considered as the maximal EMG amplitude. During the submaximal isometric tasks, the ARV was calculated for each signal over 5 s at the middle of the torque plateau. This value was normalized to the maximum ARV obtained over each of the 59 channels.

To reproduce a classical bipolar electrode configuration with the HDsEMG grids, the monopolar signals from two sets of five neighbor channels were averaged to derive an approximation of two EMG signals recorded by large electrodes (21). These two EMG signals were differentiated to obtain a bipolar derivation with an interelectrode distance of 2.4 cm. From here on out, this analysis will be referred to as bipolar HD. Similar to what was done for the HDsEMG signals, we calculated the maximal ARV of the signal over a moving time window of 250 ms during MVC. Then, we calculated the ARV over a 5-s period at the middle of the torque plateau, and we normalized this value to that determined during MVC.

We considered the ratio of normalized EMG amplitude between VL and VM to provide information about the distribution of activation between these muscles (*Eq. 1*).

$$\frac{VL}{VL + VM}\text{ratio} = \frac{\text{normalized ARV } VL}{\text{normalized } ARV\ VL + VM} \times 100 \qquad (1)$$

HDsEMG decomposition.

First, the monopolar EMG signals were bandpass filtered between 20 and 500 Hz with a second-order Butterworth filter and were visually inspected for noise and artifacts. Signals that exhibited noise or artifacts were excluded from further analysis (typically less than two signals per recording were removed). The HDsEMG signals were then decomposed using the convolutive blind source separation method (22), which is implemented in the DEMUSE tool software (v. 5.01; The University of Maribor, Slovenia). This decomposition procedure has been extensively validated using experimental and simulated signals (23, 24). All the motor unit spike trains were manually edited after the automatic identification of the motor units using the procedure described by Del Vecchio et al. (25). Specifically, after manual exclusion of spike-train segments with nonphysiological interspike intervals, the motor unit filter was updated and then applied to the entire signal to re-estimate the spike trains. Then, new spikes that were recognized by the new motor unit filter were added. It is relevant to note that all firings identified by the new filter were retained without any manual exclusion. The manual intervention only identified the most reliable signal portions for the calculation of the motor unit filters, after which the final identification of firings did not include any subjective intervention (25). Only the motor units that exhibited a pulse-to-noise ratio > 30 dB were retained for further analysis (25). This threshold ensured a sensitivity higher than 90% and a false-alarm rate lower than 2% (24).

Strength of the neural drive.

To compare the strength of neural drive received by the VL and VM muscles during the isometric knee extensions, we compared the increase in discharge rate during the ramp-up phase between VL and VM motor units with the same recruitment threshold [with a difference <0.5% of MVC; (13)]. First, we determined the recruitment threshold of each identified motor unit as the normalized joint torque at the time when the unit began to discharge (Fig. 2). The discharge rate at recruitment was considered as the mean of the first three discharges (26). Second, we determined the δ discharge rate (expressed in pps) as the rate of change in discharge rate from the recruitment to the target torque level, that is, the mean of the first three instantaneous discharge rates at the plateau level minus the discharge rate at recruitment. For each pair of matched motor units, we calculated the ratio of δ discharge rate between VL and VM using the same approach that was used for normalized EMG amplitude (*Eq. 1*). As the recruitment threshold is related to the size of the motoneuron, the matched motor units were likely to share similar excitability properties and to transform the synaptic input into action potentials in a similar way. Therefore, we considered that the ratio of δ discharge rate was an indicator of the relative strength of net excitatory input between VL and VM (13).

Common input.

If two motor units receive a common input, this will be present at the output spike train of each motor unit (20). In this way, a coherence analysis is classically performed to assess the degree of common input between motor units from the same (within-muscle coherence) or from different muscles (between-muscle coherence). This analysis represents the correlation between the two signals at given frequencies, with 0 indicating no correlation and 1 indicating a perfect correlation. Only the plateau of the three contractions was considered for the coherence analyses.

To assess the within-muscle coherence for VL and VM, we calculated the pooled coherence on two equally sized groups of cumulative spike trains (CST). The number of motor units in each of the two groups varied from one to the maximum number (half of the total number of identified units). For each iteration (number of units), all the unique combinations of motor units were tested up to a maximum of 100 random permutations. We calculated the coherence using the Welch's periodogram with nonoverlapping Hanning windows of 1 s (Fig. 3). The rate of increase in the mean coherence value over the bandwidth 0–5 Hz as a function of the number of motor units used in the calculation depends on the proportion of common synaptic input with respect to the

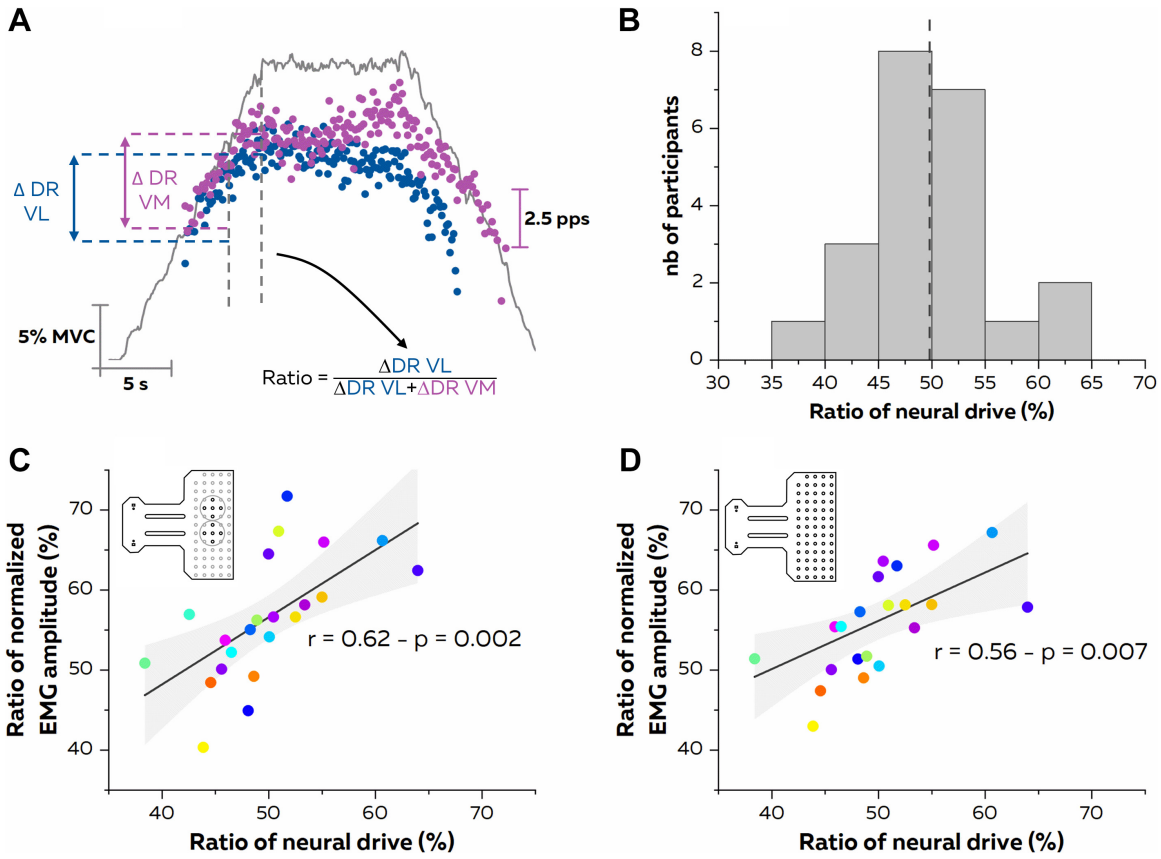

Figure 2. Distribution of the strength of neural drive between the vastus lateralis (VL) and vastus medialis (VM) muscle. *A*: to compare the strength of neural drive received by VL and VM, we compared the increase in discharge rate during the ramp-up phase between VL and VM motor units matched by recruitment threshold. *B*: group distribution of the ratio of the strength of neural drive between VL and VM (50% indicates a balanced neural drive between the muscles). *C* and *D*: relationship between the ratio of neural drive and the ratio of normalized EMG amplitude as measured using either the bipolar HD configuration (*C*) or the HDsEMG configuration (*D*). Each participant is depicted in a different color ($n = 22$). EMG, electromyography; HD, high density; HDsEMG, high-density surface electromyography; MVC, maximal isometric contractions.

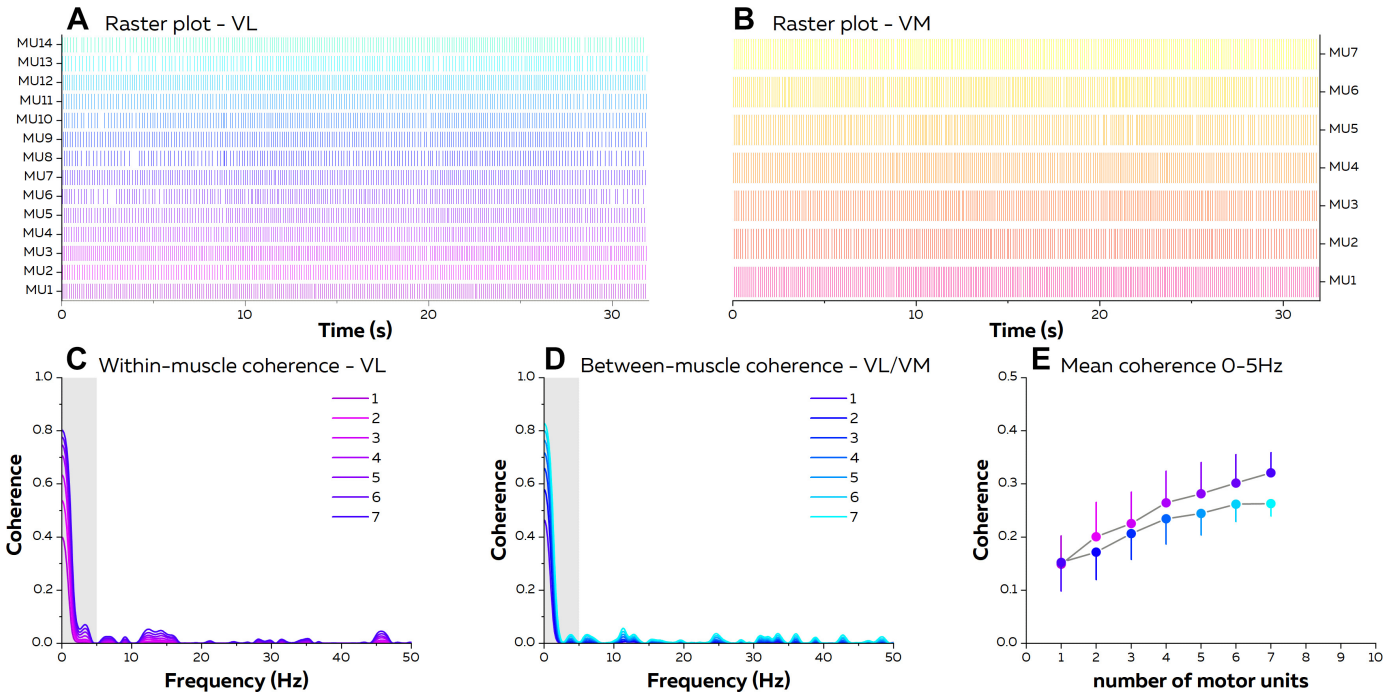

Figure 3. Calculation of the within- and between-muscle coherence. Motor unit spike trains were identified from the vastus lateralis (VL, *A*) and vastus medialis muscle (VM, *B*). For this individual example, 14 and seven motor units were identified in VL and VM, respectively. *C*: to assess the within-muscle coherence for VL and VM, we calculated the pooled coherence on two equally sized groups of cumulative spike trains (CST). The number of motor units in each of the two groups varied from 1 to the maximum number (half of the total number of identified units, i.e. seven motor units for this example—VL). *D*: to assess the between-muscle coherence, we performed pooled coherence analyses between two equally sized CST of the VM and VL muscles. The number of motor units in each CST varied from 1 to the lowest total number of identified units between VL and VM (seven for this example). *E*: change in the mean coherence in the bandwidth 0–5 Hz as a function of the number of motor units. Here, the vertical bars indicate the standard deviation across the iterations (up to 100 iterations) for a given participant. The interindividual variability was assessed from the results obtained using groups of two motor units for the within-muscle coherence and groups of three motor units for between-muscle coherence because this maximized the number of participants for whom these analyses were possible.

total input received by the motor neuron pool (27). As such, we calculated the rate of increase between group of one and group of two motor units and considered this increase as an estimate of the proportion of common input. We limited this analysis to group of two motor units, as it maximized the number of participants for whom this analysis was possible (n = 22 for VL and n = 19 for VM).

In addition, we estimated the proportion of specific drive that each muscle received with a pooled partial coherence analysis, as proposed by Laine et al. (17). The result of the partial coherence is interpreted as the level of residual coupling between each pair of motor units of a given muscle after removing the signal components that are synchronous with the neural drive of the other muscle (17, 28). Thus, the partial cross-spectra ($P_{xy/z}$) between motor units x and y accounting for the CST of the other muscle (z) was defined as:

$$P_{xy-z} = P_{xy} - \frac{P_{xz} \times P_{zy}}{P_{zz}} \quad (2)$$

where P_{xy} indicates the cross spectra between motor units x and y; P_{xz} and P_{zy} indicate the cross spectra between the CST and motor units x and y, respectively; and P_{zz} indicates the auto-spectra of the CST. The partial auto-spectra for the motor unit x (P_{xx-z}) accounting for the CST of the VM was calculated as:

$$P_{xx-z} = P_{xx} - \frac{|P_{xz}|^2}{P_{zz}} \quad (3)$$

The partial auto-spectra for the motor unit y (P_{yy-z}) was estimated similarly, and the partial coherence (COH_{xy-z}) was calculated as:

$$COH_{xy-z} = \frac{|P_{xy-z}|^2}{P_{xx-z} \times P_{yy-z}} \quad (4)$$

Finally, we calculated the ratio between the areas of the partial and total coherence within the 0–5 Hz bandwidth. We considered this value as the relative proportion of muscle-specific drive (17).

To assess the between-muscle coherence, we calculated the pooled coherence between equally sized CST of VM and VL. The number of motor units in each CST varied from 1 to the lowest total number of identified units between VL and VM. For each iteration (number of units in each CST), all unique combinations of motor units were tested up to a maximum of 100 random permutations. We calculated the coherence using the Welch's periodogram with nonoverlapping Hanning windows of 1 s. To compare the between-muscle coherence across participants, we used the results from the groups of three motor units, as it represented the minimum number of decomposed units from VM for three participants.

To account for the small difference in the duration of the signal considered for the analysis, we transformed the coherence values to a standard z-score to make comparisons between participants:

$$COH\ z\ score = \sqrt{2L} \times atanh\sqrt{COH} - bias$$

where COH is coherence, L is the number of time segments used for the coherence analysis (e.g., for 30 s, $L = 30$, as the analysis was performed on 30 windows of 1 s), and bias is the mean COH z-score between 250 and 500 Hz where no coherence is expected (29). Coherence was considered significant when the z-score was higher than 1.65 as classically used (15, 30).

Statistical Analysis

Statistical analyses were performed in Statistica v. 7.0 (StatSoft, Tulsa, OK). Distributions consistently passed the Kolmogorov–Smirnov normality test. Data are reported as means ± SD.

We first aimed to determine the individual differences in the strength of neural drive received by VL and VM and its relationship with interference EMG amplitude. To this end, the discharge rate measured at the recruitment and the rate of change in discharge rate from the recruitment to the target torque level were compared between VL and VM with separate paired t tests. The discharge rate measured at the beginning and at the end of the plateau were compared between muscles using a repeated-measures ANOVA [within-subject factor: muscle (VL, VM) and time (start plateau, end plateau)]. Normalized EMG amplitudes were compared between muscles and electrode configurations using a repeated-measures ANOVA [within-subject factor: muscle (VL, VM) and electrode configuration (bipolar HD, HDsEMG)]. The relation between the ratio of neural drive and the ratio of normalized EMG was assessed using the Pearson's correlation coefficient.

Second, we aimed to determine the individual differences in the degree of common input to the motor neuron pools innervating each muscle and between pools innervating the two muscles. Mean and maximal coherence within the δ band (0–5 Hz), proportion of common input, and muscle-specific drive were compared between VL and VM using separate paired t tests. The relationship between the within-muscle and the between-muscle coherence over the δ band was estimated with the Pearson's correlation coefficient. To investigate the relationship between task performance and the degree of common input, we calculated the Pearson's correlation coefficient between the coefficient of variation of torque and the mean coherence within the δ band.

To investigate the consistency of neural strategies over time, we calculated the intraclass correlation coefficient (ICC) and the standard error of measurement (SEM) between the two sessions. We performed this analysis on the δ discharge rate, the ratio of neural drive, and the ratio of normalized EMG amplitude for the first aim. We estimated the consistency of the mean within-muscle and between-muscle coherence in the 0–5 Hz bandwidth and the muscle-specific drive for the second aim. ICC with values less than 0.4, between 0.4 and 0.6, between 0.6 and 0.75, and greater than 0.75 were considered poor, fair, good, and excellent, respectively (31). The level of significance was set at $P < 0.05$.

RESULTS

The entire data set (raw and processed data) is available at https://doi.org/10.6084/m9.figshare.12739133.

Motor Unit Decomposition

The total number of decomposed motor units was 302 and 174 for VL and VM, respectively. This resulted in an average number of decomposed motor units per participant of 13.7 ± 4.9 for VL (range: 4–23) and 7.9 ± 2.9 (range: 3–14) for VM. For the aims of this study, only motor units with specific recruitment thresholds (a matched threshold between VL and VM, *aim 1*) or with enough number of discharges (a continuous discharge for >25 s; *aim 2*) were selected.

Distribution of the Strength of Neural Drive between VL and VM

To compare the strength of neural drive received by the two muscles, we compared the rate of increase in discharge rate between VL and VM motor units, which were matched based on their recruitment threshold (Fig. 2*A*). A total of 176 motor units were matched between VL and VM, with an average of 8 ± 4.3 units per participant (range: 2–21). Their average recruitment threshold was 13.7 ± 3.3% of MVC. The mean discharge rate of these matched motor units at recruitment was lower for VL (5.9 ± 1.4 pps) than for VM (6.5 ± 1.2 pps; $P = 0.002$). The mean discharge rate during the torque plateau was also lower for VL than VM (main effect of muscle: $P < 0.001$) and decreased between the start and the end of the plateau regardless of the muscle (main effect of time: $P < 0.001$). There was not significant interaction between muscle and time ($P = 0.92$). It should be noted that when all of the identified motor units were considered, there was no significant difference in discharge rate during the plateau between VL and VM [VL ($n = 302$): 9.4 ± 1.6 pps versus VM ($n = 174$): 9.8 ± 1.5 pps; $P = 0.10$].

At the group level, the δ discharge rate between recruitment and target torque did not differ between muscles (VL: 3.7 ± 1.1 pps versus VM: 3.8 ± 1.2 pps; $P = 0.62$), resulting in a mean VL/(VL + VM) ratio of 49.7 ± 5.8%. However, inspection of individual participants revealed a large interindividual variability with the VL/(VL + VM) ratio ranging from 38.6% to 64.0% (Fig. 2).

Six out of the 22 participants underwent a second experimental session ~20 mo after the initial session to test the consistency of the outcome measures. ICC values for the rate of increase in discharge rate were good for VL (ICC = 0.71) and were fair for VM (ICC = 0.51), with SE values of 0.61 and 0.66 pps for VL and VM, respectively. The ICC value for the VL/(VL + VM) ratio of neural drive was fair (ICC = 0.46), and the SE value was relatively low (SE = 4%).

Relationship between Interference EMG and Neural Drive

Normalized interference EMG amplitude was significantly higher for VL than VM regardless of the electrode configuration (main effect of muscle: $P < 0.001$), resulting in a VL/(VL + VM) ratio of 56.4 ± 7.8% and 56.0 ± 6.2% of maximal EMG ARV for the bipolar HD and HDsEMG configuration,

respectively. Of note, normalized EMG amplitude was higher for the HDsEMG configuration than for the bipolar HD configuration (main effect of electrode configuration: $P < 0.001$), but values were well correlated between these two configurations ($r = 0.77$ and $P < 0.001$ for VL; $r = 0.94$ and $P < 0.001$ for VM). Similar to what was observed for the distribution of neural drive, there was a large interindividual variability for the VL/(VL + VM) ratios, ranging from 40.4% to 71.7% for the bipolar HD configuration and from 43.0% to 67.2% for the HDsEMG configuration. Interestingly, the between-session reliability of the distribution of normalized EMG amplitude [VL/(VL + VM) ratio] tested on the six participants was good (ICC = 0.74 and SE = 5%) and excellent (ICC = 0.96 and SE = 2%) for the bipolar HD and the HDsEMG configuration, respectively. Overall, these results suggest that the distribution in normalized EMG amplitude was consistent between sessions.

There was a significant positive correlation between the ratio of neural drive and the ratio of normalized EMG amplitude [$r = 0.62$ and $P = 0.002$ for the bipolar HD configuration (Fig. 2*C*); $r = 0.56$ and $P = 0.007$ for the HD-EMG configuration (Fig. 2*D*)].

Within- and Between-Muscle Coherence

After discarding the motor units that were not recruited during all of the three contractions and removing the data from participants with less than four consistently firing motor units (three participants for VM), the within-muscle coherence analysis was performed on 265 motor units from 22 participants for VL and on 134 motor units from 19 participants for VM. It resulted in an average of 12 ± 4 and 7.1 ± 1.8 motor units for VL and VM, respectively. The between-muscle coherence analysis was performed on 12 ± 4 motor units for VL and 6.5 ± 2.2 motor units for VM from the 22 participants. On average, the coherence analysis was performed on signals of 29 ± 1 s duration. Note that the coefficient of variation of the torque produced during the plateau ranged from 1.1% to 3.1%, meaning that all the participants were able to track the target without difficulty. There was no significant relationship between the coefficient of variation of the torque and any values of coherence (range: $r = -0.21$ to 0.26).

The index of the proportion of common synaptic input (PCI), with respect to the total input received by the motor neuron pool of each muscle, was estimated from the relationship between the mean coherence over the bandwidth 0–5 Hz and the number of motor units used to calculate this coherence (Fig. 4, *A* and *B*). Interindividual differences in the mean coherence increased with the number of motor units considered in the analysis (Fig. 4, *A* and *B*). The rate of increase calculated between group of one and group of two motor units, for which most of the participants could be considered in the analysis, did not differ between muscles ($P = 0.19$). Inspection of data for individual participants revealed a variability in the overall rate of increase and, thus, in the estimated proportion of common input (Fig. 4, *A* and *B*).

Figure 5 depicts the within-muscle coherence calculated for the combinations of all the unique pairs of motor units (e.g., a group of one motor unit from the aforementioned analysis). The overall coherence profiles were similar between muscles, with the highest coherence being observed within the 0–5 Hz bandwidth (δ band), and more specifically below 2 Hz. No significant coherence was observed within the α (5–15 Hz) and β band (15–35 Hz). The coherence calculated over the δ band did not differ between muscles, regardless of whether we considered the mean ($P = 0.19$) or the maximal value ($P = 0.11$). A total of 82% and 95% of the participants exhibited a significant within-muscle coherence for at least one frequency within the 0–5 Hz bandwidth for VL and VM, respectively.

The level of between-muscle coherence increased with the number of motor units considered in the analysis for most, but not all, of the participants (Fig. 4). To compare the between-muscle coherence across individuals, we considered the results from group of three motor units because this represented the minimum number of identified motor units in VM for three participants. Even though most of the participants exhibited a significant coherence between VL and VM over the entire bandwidth 0–5 Hz, others exhibited little coherence, with one participant not reaching the level of significance for any of the frequencies (Fig. 4*C*). Of note, three of 22 and one of 22 participants exhibited a significant coherence within the α and β band, respectively. The mean between-muscle coherence in the 0–5 Hz bandwidth was positively correlated with the mean within-muscle coherence in the 0–5 Hz bandwidth of either VL ($r = 0.49$, $P = 0.021$; Fig. 6*A*) or VM ($r = 0.58$, $P = 0.009$; Fig. 6*B*). This indicates that the participants who exhibited a large coherence between motor units of the same muscle also exhibited a large coherence between muscles. This was further confirmed by the positive correlation between the mean between-muscle coherence in the 0–5 Hz bandwidth and the index of the proportion of common input ($r = 0.56$, $P = 0.007$, and $r = 0.56$, $P = 0.012$, for VL and VM, respectively). The same analyses were performed on the 1.5–5 Hz bandwidth to confirm that the high magnitude of coherence below 1.5 Hz did not influence the outcomes. The mean coherence values were highly correlated to those obtained over the 0–5 Hz bandwidth (r values for VL = 0.87; r values for VM = 0.95), and the relationships between the within- and between-muscle coherence were still significant ($r = 0.79$ and $r = 0.72$ for VL and VM, respectively).

The reliability of the mean within-muscle coherence in the 0–5 Hz bandwidth (z-score) was excellent for VL (ICC = 0.93; SE = 0.21) and fair for VM (ICC = 0.45; SE = 0.69). We also found an excellent reliability (ICC = 0.91; SE = 0.62) for the mean between-muscle coherence in the 0–5 Hz bandwidth (z-score). Inspection of Fig. 7 emphasizes the similarity of the shapes of coherence curves between the two sessions, even when data collection is interspaced by 20 mo. The reliability analysis rules out the possibility that the interindividual variation of common input observed in this study depended solely on the variability of the measures.

Muscle-Specific Drive

To estimate the muscle-specific drive, we calculated the within-muscle coherence after removing the CST of the other muscle, that is, partial coherence (Fig. 8*A*). The partial coherence represented the muscle-specific drive, that is, the drive that was not shared with the other recorded synergist muscle. Figure 8 depicts the ratio between the partial and

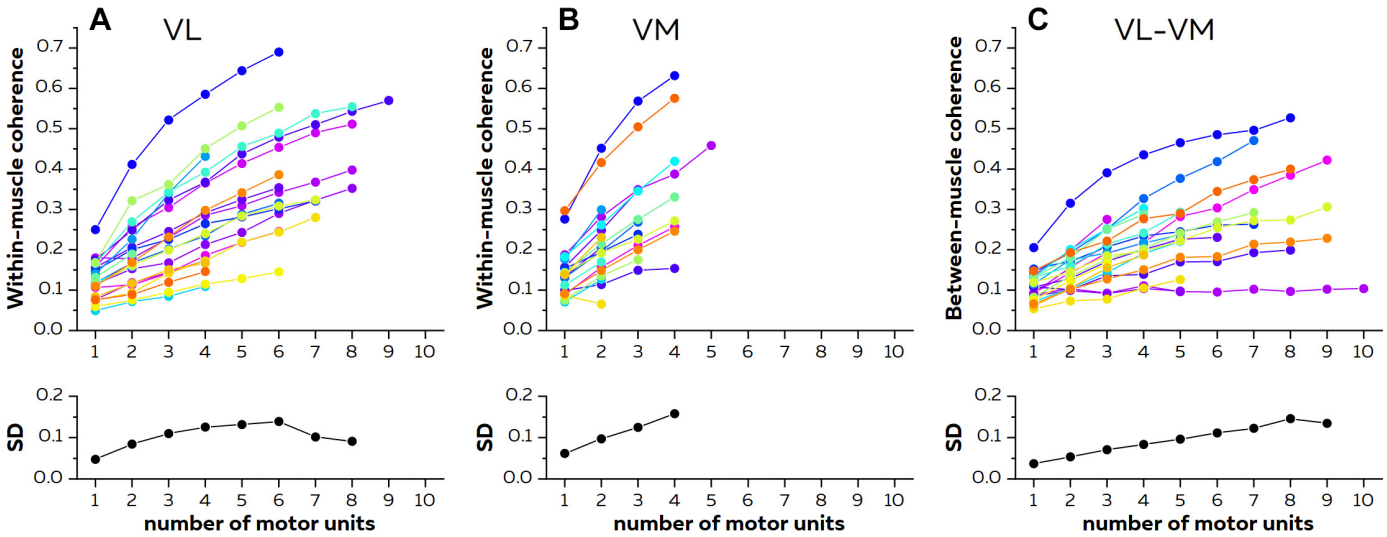

Figure 4. Relationship between the mean coherence in the δ band and the number of motor units considered in the analysis. Each panel represents the relationship between the mean values of coherence in the bandwidth 0–5 Hz (within-muscle for *A* and *B*, between-muscles for *C*) and the number of motor units. The coherence analyses were performed on two cumulative spike trains, with a varying number of motor units in each group. Each estimation is the average of the permutations of all possible combinations of group of motor units, or after the completion of 100 permutations. Each participant is depicted in a different color. The lower panels depict the standard deviation (SD) across participants. Note that the drops at the highest number of motor units can be explained by the lower number of participants used to calculate the SD. VL, vastus lateralis; VM, vastus medialis.

the pooled coherence, which was considered as the proportion of muscle-specific drive. On average, the percentage of muscle-specific drive was 37 ± 24% for VL and 41 ± 23% for VM, with no significant difference between muscles (P = 0.77). Again, a large interindividual variability was observed with values ranging from 6% to 83% for VL (Fig. 8*B*) and from 6% to 86% for VM (Fig. 8*C*). The percentage of muscle-specific drive was positively correlated between VL and VM (r = 0.82; $P < 0.001$), and, as expected, was negatively correlated with the mean between-muscle coherence within the

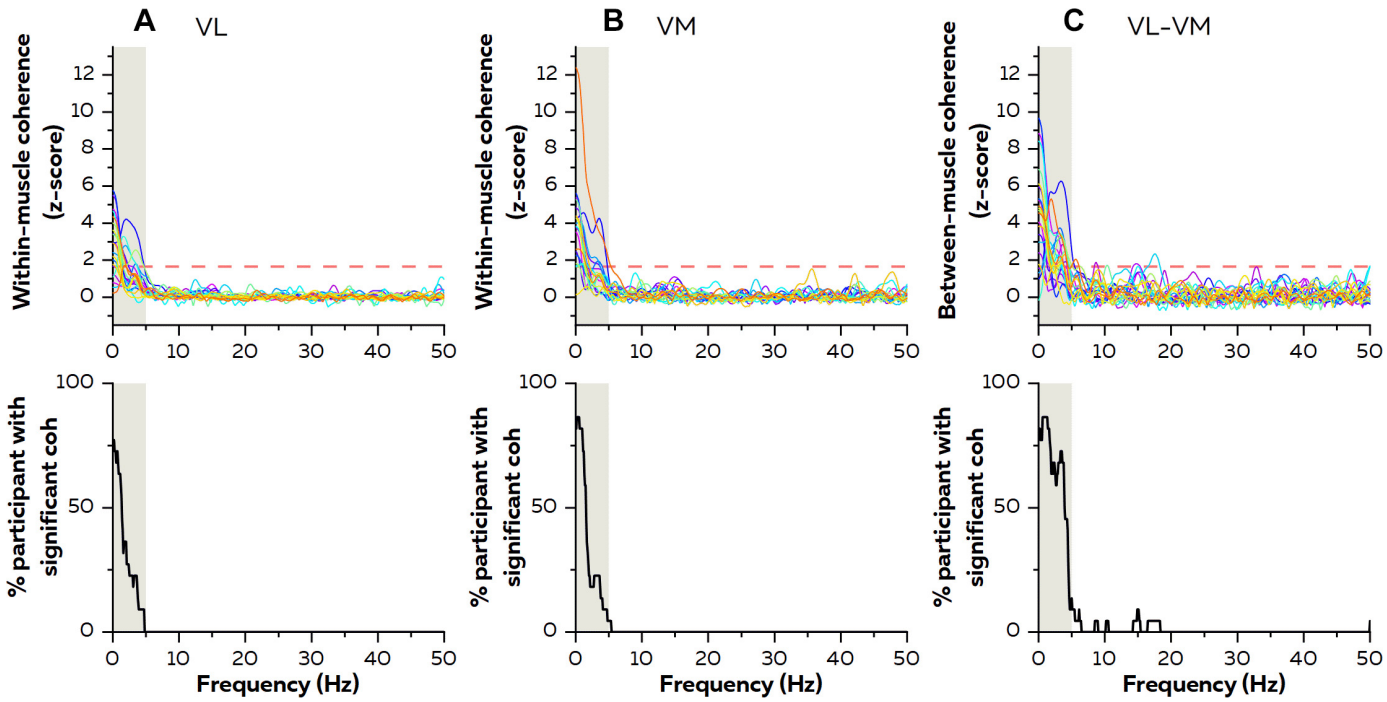

Figure 5. Within- and between-muscle coherence. The within-muscle coherence (*z*-score) is depicted for each participant on the *top* [*A*: VL (n = 22); *B*: VM (n = 19)]. The coherence (*z*-score) between VL and VM is depicted in *C*. The red horizontal dashed line indicates the significant threshold, which is set at 1.65. The *bottom* indicates the percentage of participants who exhibited a significant coherence. Note that comparison of absolute values from within-muscle and between-muscle coherences should be performed with caution, as we considered pairs of motor units for the within-muscle coherence and cumulative spike trains of three motor units for the between-muscle coherence. VL, vastus lateralis; VM, vastus medialis.

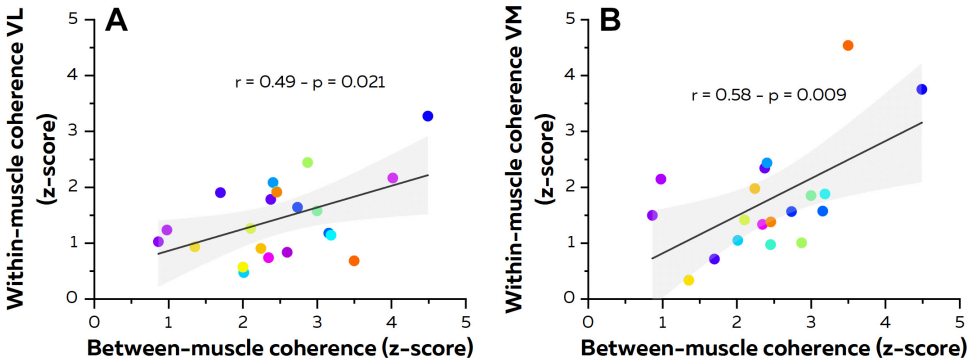

Figure 6. Relationship between the within- and between-muscle coherence. The analysis was performed using the mean coherence values (*z*-score) in the bandwidth 0–5 Hz. Each participant is depicted in a different color. Note that comparison of absolute values from within-muscle and between-muscle coherences should be performed with caution, as the number of motor units considered for these analyses was different (see METHODS). VL, vastus lateralis; VM, vastus medialis.

0–5 Hz bandwidth (VL: $r = -0.64$, $P = 0.001$; VM: $r = -0.49$, $P = 0.031$). Of note, similar results were observed when calculating the muscle-specific drive only from frequencies with significative coherence. Finally, the reliability of muscle-specific drive was excellent for both the VL (ICC = 0.89; SE = 14%) and the VM muscle (ICC = 0.91; SE = 14%).

DISCUSSION

The distribution of the strength of neural drive between VL and VM and the degree of common input to the motor neuron pools within and between these muscles varied across individuals, even during a highly constrained motor task. Importantly, these strategies were robust across sessions that were interspaced by 20 mo. Together, these results provide strong evidence of the existence of individual neural strategies to control the VL and VM muscles. Understanding the reasons and the consequences of these individual differences is important to expand our understanding of muscle control in health and disease.

Strength of Neural Drive

Because EMG amplitude provides a crude index of neural drive (11, 12), it remains unclear to what extent the observed individual differences in the distribution of normalized EMG amplitude across synergist muscles (5, 9, 32) reflect differences in neural control strategies. As proposed by Martinez-Valdes et al. (13), we assessed the strength of neural drive by

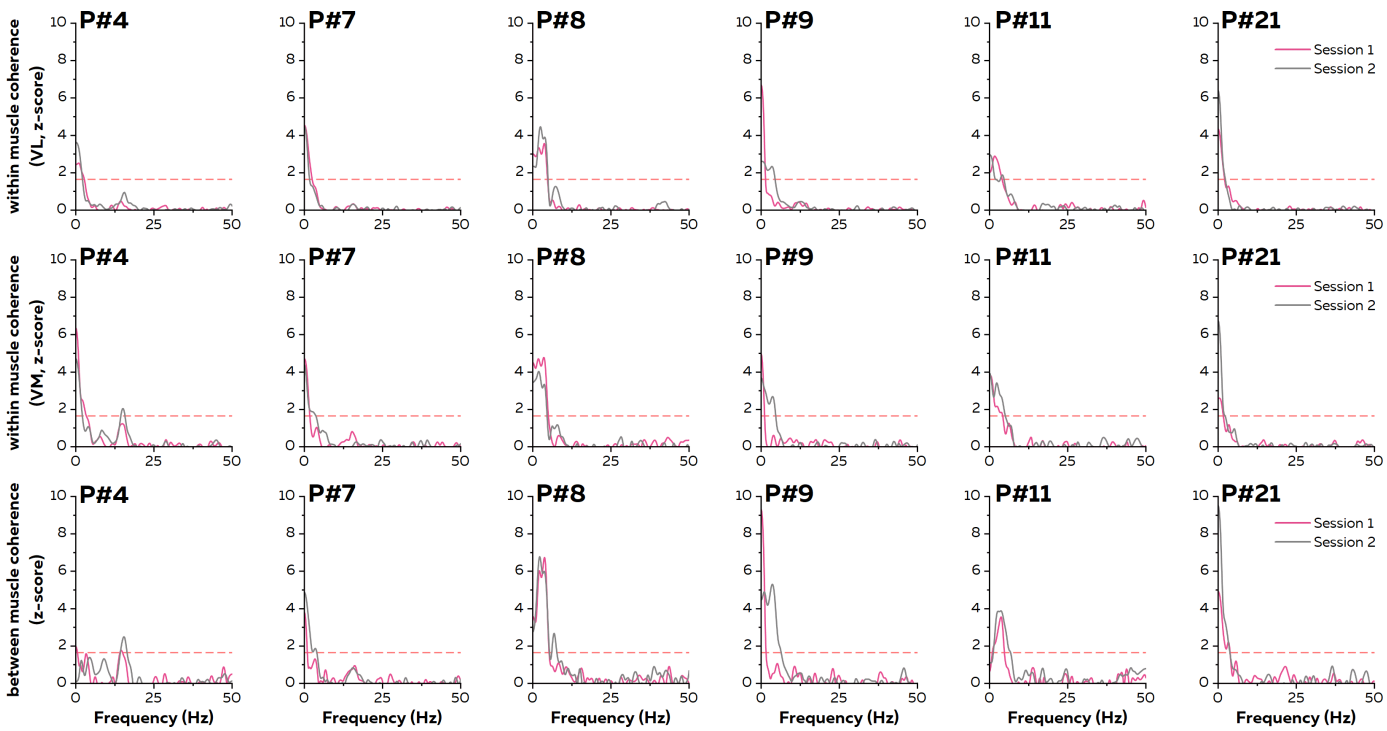

Figure 7. Reliability of within- and between- muscle coherence over a 20-mo period. Each panel depicts the coherence analysis performed in *session 1* and *session 2* for six participants. The within-muscle coherence (*z*-score) is depicted in the *top* for VL and in the *middle* for VM. The between-muscle coherence (*z*-score) is depicted in the *bottom*. The red horizontal dashed line indicates the significant threshold, which was set at 1.65. Of note, *participant 4* exhibited negligible coherence between VL and VM. The fact that this uncommon behavior was consistently observed across sessions made us confident that this was actually related to a specific individual neural strategy. VL, vastus lateralis; VM, vastus medialis.

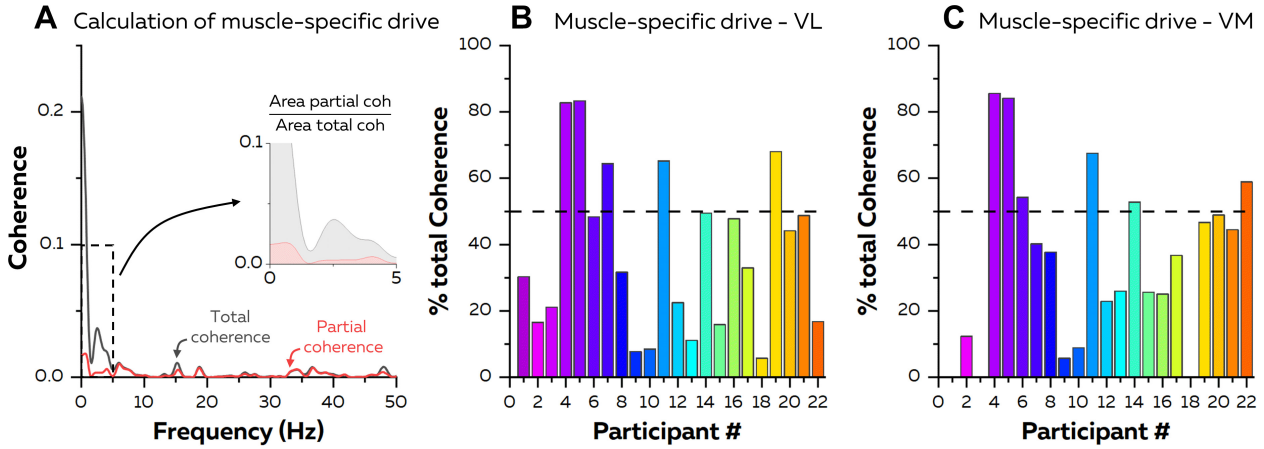

Figure 8. Muscle-specific drive. *A*: the total coherence was calculated as the pooled coherence between the cumulative spike trains (CST) of all the unique pairs of motor units, or after completing 100 iterations. We also calculated the within-muscle coherence after removing the CST of the other muscle (partial coherence). We considered the ratio between areas of the partial and total coherences over the 0–5 Hz bandwidth as the relative proportion of muscle-specific drive. *B* and *C*: relative proportion of muscle-specific drive for VL (*B*) and VM (*C*). Note that this analysis was performed on 19 participants for VM, because less than four motor units were identified in three of the participants for this muscle. VL, vastus lateralis; VM, vastus medialis.

calculating the increase in discharge rate from recruitment to target torque. To ensure that we compared VL and VM motor units with similar intrinsic properties, this analysis was performed on motor units matched by recruitment threshold. In accordance with previous work (13), the analysis performed at the group level suggested that the VL and VM muscles received similar levels of synaptic input despite the fact that a greater normalized EMG amplitude was observed for VL compared with VM. However, inspection of individual data revealed a large interindividual variability in the distribution of neural drive (Fig. 2*B*), with 11 participants exhibiting a stronger drive to the VL muscle and 11 participants exhibiting a lower drive to the VL muscle [range of VL/(VL + VM) ratio: 39%–64%]. Interestingly, there was a significant positive correlation between the ratio of neural drive and the ratio of normalized EMG amplitude. Even though the normalized interference EMG does not provide a direct quantification of the neural drive, our results suggest that individual differences in the distribution of normalized EMG between synergist muscles reflect actual differences in the distribution of neural drive. These results may contribute to interpreting interindividual differences in the interference EMG data.

It is important to note that the reproducibility of the ratios of neural drive assessed 20 mo apart was only fair (ICC = 0.46; SE = 4%). Even though this result could be explained by the relatively low number of paired motor units, the positive correlation between this index and the ratio of normalized EMG amplitude makes us confident that the observed variability between participants was explained, at least in part, by variability in the distribution of neural drive.

Common Input

The synaptic input received by pools of motor neurons innervating the same or different muscles is composed of common and independent inputs (14, 27, 33–35). The common input generates the effective neural drive responsible for the control of muscle force (20, 36–38), whereas the independent input is mostly filtered out in the generation of the neural drive. Here, we applied a coherence analysis to assess the degree of common input between motor units from the same (within-muscle coherence) or from different muscles (between-muscle coherence). Our results confirmed the presence of significant within- and between-muscle coherence within the 0–5 Hz bandwidth. This is in accordance with the model proposed by Laine et al. (17), where the VL and VM muscles receive both common and unique inputs. However, in this work, we measured a substantially larger sample of individuals than in previous work, and this allowed us to investigate the relationship between different outcomes. We observed a positive correlation between the level of within- and between-muscle coherence (Fig. 6), suggesting that the within-muscle coherence is largely influenced by the level of common drive between muscles. As such, the measure of within-muscle coherence provides information about all the levels of between-muscle coherence. Although it is tempting to conclude that the within-muscle coherence could be used as a surrogate of the common drive shared between synergist muscles, this does not hold true for all muscles. For example, even though a high level of within-muscle coherence was observed on the gastrocnemius muscles, the between-muscle coherence between these muscles was very low (39).

To further assess the degree of common input between VL and VM, we calculated the within-muscle coherence after removing the CST of the other muscle, and we considered this partial coherence to be representative of the muscle-specific drive. In accordance with Laine et al. (17), we observed that the proportion of muscle-specific drive over the total drive was relatively low (37 ± 24% for VL and 41 ± 23% for VM), confirming that these two synergist muscles share most of their drive. However, it is important to note that this conclusion is only true "on average." Inspection of data for individual participants revealed that the proportion of muscle-specific drive varied greatly between participants, with a logical negative correlation between the common drive between muscles (mean coherence between 0 and 5 Hz) and the

proportion of muscle-specific drive (VL: $r = -0.65$; $P = 0.001$; VM: $r = -0.48$, $P = 0.031$). Interestingly, in contrast to previous results (17), we observed that some participants (e.g., *participants 4*, *5*, and *11*) exhibited very little coherence between VL and VM, leading to a proportion of muscle-specific drive greater than 80% in two participants. To the best of our knowledge, this is the first report of an interindividual variability in the coherence values within and between synergist muscles. To interpret this variability as a physiological variability related to the amount of common input received by these muscles, it was important to rule out the possibility that this variability originated from the experimental and/or analysis procedures. First, to be representative of common input received by motor neuron pools, it is important that the coherence analysis is performed on several motor units (27). This is because the level of coherence increases monotonically with the number of units used for the analysis (36), as shown in Fig. 4. Importantly, a low level of coherence was observed in participants with a relatively large number of decomposed units (e.g., *participant 4*: 22 and 14 motor units for VL and VM, respectively). Second, six participants were retested ~20 mo after the first session, and coherence values were highly reproducible. For example, *participant 4* exhibited very little coherence between VL and VM for both sessions (Fig. 7). Together, these observations gave us confidence that the variability of the outcome measures reflected variability in the degree of common input rather than measurement noise.

Of note, the neural drive to the muscles appeared to be limited to the common drive [0–5 Hz (34)], with only four participants exhibiting a significant coherence above 5 Hz. This is in contrast with the observation that there is a significant coherence in the α and β bands made in other muscles [e.g., hand muscles (16)]. Even though a variety of factors can limit the sensitivity of the coherence measures (40), our results suggest a lower influence from the supraspinal and afferent inputs in musculature involved in force production in opposition of muscles involved in fine motor tasks.

Origin and Consequences of Individual Strategies

The origin of the interindividual differences in the neural control of VL and VM is unclear. It is possible that differences in neural circuitries are shaped by developmental processes, motor exploration, experience, and training (3). Central pattern generators are capable of learning and adaptation, which may lead to interindividual variability in movement behavior (41). Because movement results from the interplay between neural strategies and the properties of the neuromusculoskeletal system (4), it is possible that the neural strategies adapt to individual mechanical properties. This is in agreement with indirect observations obtained from interference EMG, indicating that muscle activation is biased by muscle force-generating capacity, that is, the greater the force-generating capacity of VL compared with VM, the stronger bias of activation to the VL (10). Even though this coupling might explain the large range of ratios of neural drive (Fig. 2), it does not explain the interindividual variability in the level of common drive between VL and VM. Variations in common drive can arise from the proprioceptive feedback loops. Thus, several studies have reported an inverse relationship between the strength of reflex response due to the activation of afferent fibers and the degree of common drive (42, 43). In this way, the balance of Ia afferent gains could differ between VL and VM (44) in subject-specific manner, which in turn could impact the degree of common drive.

The coordination of VL and VM plays an important role in regulating the internal joint stress (45). As such, a relatively large common drive between these muscles, as observed in a majority of our participants, might be an efficient strategy to prevent knee injury and might explain why activation of VL and VM cannot be voluntary disassociated (46). This logically leads to the question of what the functional impact of a low common drive between VL and VM is, as observed in a small subset of our participants. In line with the role of VL and VM in minimizing the joint stress, a lower common drive might be associated with a higher risk of developing knee-related injuries. In this way, Mellor and Hodges (47) observed a lower synchronization between VL and VM motor units in people with anterior knee pain. Of note, our study did not consider the different portions of the VM muscle (longus and obliques). Future studies should explore potential differences between the different portions of the VM muscle. Finally, the level of common drive between these muscles may influence the ability to disassociate the activation of the VL and VM muscles, which might, in some situations, be beneficial (e.g., compensation during a fatiguing task). Overall, these results provide the motivation to determine the functional consequences of the individual neural strategies.

GRANTS

F. Hug is supported by a fellowship from the Institut Universitaire de France (IUF). Support was received from the French national research agency (ANR-19-CE17-002-01, COMMODE project; to F. Hug) and from the European Research Council Synergy Grant NaturalBionicS (Contract No. 810346; to D. Farina).

DISCLOSURES

No conflicts of interest, financial or otherwise, are declared by the authors.

AUTHOR CONTRIBUTIONS

S.A., A.D., D.F., C.V., J.U., and F.H. conceived and designed research; S.A., C.V., and J.U. performed experiments; S.A., A.D., C.V., and F.H. analyzed data; S.A., A.D., D.F., J.L.P., and F.H. interpreted results of experiments; S.A. prepared figures; S.A. and F.H. drafted manuscript; S.A., A.D., D.F., J.L.P., J.U., and F.H. edited and revised manuscript; S.A., A.D., D.F., J.L.P., C.V., J.U., and F.H. approved final version of manuscript.

ENDNOTE

At the request of the authors, readers are herein alerted to the fact that the entire data set (raw and processed data) is available at https://doi.org/10.6084/m9.figshare.12739133. These materials are not a part of this manuscript and have not undergone peer review by the American Physiological Society (APS). APS and the journal editors take no responsibility

for these materials, for the website address, or for any links to or from it.

REFERENCES

1. **Horst F**, **Lapuschkin S**, **Samek W**, **Muller KR**, **Schollhorn WI.** Explaining the unique nature of individual gait patterns with deep learning. *Sci Rep* 9: 2391, 2019. doi:10.1038/s41598-019-38748-8.
2. **Hug F**, **Vogel C**, **Tucker K**, **Dorel S**, **Deschamps T**, **Le Carpentier E**, **Lacourpaille L.** Individuals have unique muscle activation signatures as revealed during gait and pedaling. *J Appl Physiol (1985)* 127: 1165–1174, 2019. doi:10.1152/japplphysiol.01101.2018.
3. **Ting LH**, **Chiel HJ**, **Trumbower RD**, **Allen JL**, **McKay JL**, **Hackney ME**, **Kesar TM.** Neuromechanical principles underlying movement modularity and their implications for rehabilitation. *Neuron* 86: 38–54, 2015. doi:10.1016/j.neuron.2015.02.042.
4. **Tytell ED**, **Holmes P**, **Cohen AH.** Spikes alone do not behavior make: why neuroscience needs biomechanics. *Curr Opin Neurobiol* 21: 816–822, 2011. doi:10.1016/j.conb.2011.05.017.
5. **Ahn AN**, **Kang JK**, **Quitt MA**, **Davidson BC**, **Nguyen CT.** Variability of neural activation during walking in humans: short heels and big calves. *Biol Lett* 7: 539–542, 2011. doi:10.1098/rsbl.2010.1169.
6. **Arsenault AB**, **Winter DA**, **Marteniuk RG.** Is there a 'normal' profile of EMG activity in gait? *Med Biol Eng Comput* 24: 337–343, 1986. doi:10.1007/BF02442685.
7. **Hug F**, **Turpin NA**, **Guevel A**, **Dorel S.** Is interindividual variability of EMG patterns in trained cyclists related to different muscle synergies? *J Appl Physiol (1985)* 108: 1727–1736, 2010. doi:10.1152/japplphysiol.01305.2009.
8. **Pedotti A.** A study of motor coordination and neuromuscular activities in human locomotion. *Biol Cybernetics* 26: 53–62, 1977. doi:10.1007/BF00363992.
9. **Crouzier M**, **Hug F**, **Dorel S**, **Deschamps T**, **Tucker K**, **Lacourpaille L.** Do individual differences in the distribution of activation between synergist muscles reflect individual strategies? *Exp Brain Res* 237: 625–635, 2019. doi:10.1007/s00221-018-5445-6.
10. **Hug F**, **Goupille C**, **Baum D**, **Raiteri BJ**, **Hodges PW**, **Tucker K.** Nature of the coupling between neural drive and force-generating capacity in the human quadriceps muscle. *Proc Biol Sci* 282: 20151908, 2015. doi:10.1098/rspb.2015.1908.
11. **Dideriksen JL**, **Enoka RM**, **Farina D.** Neuromuscular adjustments that constrain submaximal EMG amplitude at task failure of sustained isometric contractions. *J Appl Physiol (1985)* 111: 485–494, 2011. doi:10.1152/japplphysiol.00186.2011.
12. **Enoka RM**, **Duchateau J.** Inappropriate interpretation of surface EMG signals and muscle fiber characteristics impedes understanding of the control of neuromuscular function. *J Appl Physiol (1985)* 119: 1516–1518, 2015. doi:10.1152/japplphysiol.00280.2015.
13. **Martinez-Valdes E**, **Negro F**, **Falla D**, **De Nunzio AM**, **Farina D.** Surface electromyographic amplitude does not identify differences in neural drive to synergistic muscles. *J Appl Physiol (1985)* 124: 1071–1079, 2018. doi:10.1152/japplphysiol.01115.2017.
14. **Farmer SF**, **Bremner FD**, **Halliday DM**, **Rosenberg JR**, **Stephens JA.** The frequency content of common synaptic inputs to motoneurones studied during voluntary isometric contraction in man. *J Physiol* 470: 127–155, 1993. doi:10.1113/jphysiol.1993.sp019851.
15. **Laine CM**, **Valero-Cuevas FJ.** Intermuscular coherence reflects functional coordination. *J Neurophysiol* 118: 1775–1783, 2017. doi:10.1152/jn.00204.2017.
16. **Del Vecchio A**, **Germer CM**, **Elias LA**, **Fu Q**, **Fine J**, **Santello M**, **Farina D.** The human central nervous system transmits common synaptic inputs to distinct motor neuron pools during non-synergistic digit actions. *J Physiol* 597: 5935–5948, 2019. doi:10.1113/JP278623.
17. **Laine CM**, **Martinez-Valdes E**, **Falla D**, **Mayer F**, **Farina D.** Motor neuron pools of synergistic thigh muscles share most of their synaptic input. *J Neurosci* 35: 12207–12216, 2015. doi:10.1523/JNEUROSCI.0240-15.2015.
18. **Castronovo AM**, **Mrachacz-Kersting N**, **Stevenson AJT**, **Holobar A**, **Enoka RM**, **Farina D.** Decrease in force steadiness with aging is associated with increased power of the common but not independent input to motor neurons. *J Neurophysiol* 120: 1616–1624, 2018. doi:10.1152/jn.00093.2018.
19. **Feeney DF**, **Mani D**, **Enoka RM.** Variability in common synaptic input to motor neurons modulates both force steadiness and pegboard time in young and older adults. *J Physiol* 596: 3793–3806, 2018. doi:10.1113/JP275658.
20. **Farina D**, **Negro F**, **Dideriksen JL.** The effective neural drive to muscles is the common synaptic input to motor neurons. *J Physiol* 592: 3427–3441, 2014. doi:10.1113/jphysiol.2014.273581.
21. **Del Vecchio A**, **Negro F**, **Felici F**, **Farina D.** Associations between motor unit action potential parameters and surface EMG features. *J Appl Physiol (1985)* 123: 835–843, 2017. doi:10.1152/japplphysiol.00482.2017.
22. **Holobar A**, **Zazula D.** Multichannel blind source separation using convolution kernel compensation. *IEEE Trans Signal Process* 55: 4487–4496, 2007. doi:10.1109/TSP.2007.896108.
23. **Holobar A**, **Farina D.** Blind source identification from the multichannel surface electromyogram. *Physiol Meas* 35: R143–165, 2014. doi:10.1088/0967-3334/35/7/R143.
24. **Holobar A**, **Minetto MA**, **Farina D.** Accurate identification of motor unit discharge patterns from high-density surface EMG and validation with a novel signal-based performance metric. *J Neural Eng* 11: 016008, 2014. doi:10.1088/1741-2560/11/1/016008.
25. **Del Vecchio A**, **Holobar A**, **Falla D**, **Felici F**, **Enoka RM**, **Farina D.** Tutorial: analysis of motor unit discharge characteristics from high-density surface EMG signals. *J Electromyogr Kinesiol* 53: 102426, 2020. doi:10.1016/j.jelekin.2020.102426.
26. **Farina D**, **Holobar A**, **Gazzoni M**, **Zazula D**, **Merletti R**, **Enoka RM.** Adjustments differ among low-threshold motor units during intermittent, isometric contractions. *J Neurophysiol* 101: 350–359, 2009. doi:10.1152/jn.90968.2008.
27. **Farina D**, **Negro F**, **Muceli S**, **Enoka RM.** Principles of motor unit physiology evolve with advances in technology. *Physiology (Bethesda)* 31: 83–94, 2016. doi:10.1152/physiol.00040.2015.
28. **Halliday DM**, **Rosenberg JR**, **Amjad AM**, **Breeze P**, **Conway BA**, **Farmer SF.** A framework for the analysis of mixed time series/point process data–theory and application to the study of physiological tremor, single motor unit discharges and electromyograms. *Prog Biophys Mol Biol* 64: 237–278, 1995. doi:10.1016/S0079-6107(96)00009-0.
29. **Baker SN**, **Pinches EM**, **Lemon RN.** Synchronization in monkey motor cortex during a precision grip task. II. Effect of oscillatory activity on corticospinal output. *J Neurophysiol* 89: 1941–1953, 2003. doi:10.1152/jn.00832.2002.
30. **Rosenberg JR**, **Amjad AM**, **Breeze P**, **Brillinger DR**, **Halliday DM.** The Fourier approach to the identification of functional coupling between neuronal spike trains. *Prog Biophys Mol Biol* 53: 1–31, 1989. doi:10.1016/0079-6107(89)90004-7.
31. **Cicchetti D**, **Bronen R**, **Spencer S**, **Haut S**, **Berg A**, **Oliver P**, **Tyrer P.** Rating scales, scales of measurement, issues of reliability: resolving some critical issues for clinicians and researchers. *J Nerv Ment Dis* 194: 557–564, 2006. doi:10.1097/01.nmd.0000230392.83607.c5.
32. **Avrillon S**, **Guilhem G**, **Barthelemy A**, **Hug F.** Coordination of hamstrings is individual specific and is related to motor performance. *J Appl Physiol (1985)* 125: 1069–1079, 2018. doi:10.1152/japplphysiol.00133.2018.
33. **Boonstra TW**, **Farmer SF**, **Breakspear M.** Using computational neuroscience to define common input to spinal motor neurons. *Front Hum Neurosci* 10: 313, 2016.
34. **De Luca CJ**, **Erim Z.** Common drive in motor units of a synergistic muscle pair. *J Neurophysiol* 87: 2200–2204, 2002. doi:10.1152/jn.00793.2001.
35. **Nordstrom MA**, **Fuglevand AJ**, **Enoka RM.** Estimating the strength of common input to human motoneurons from the cross-correlogram. *J Physiol* 453: 547–574, 1992. doi:10.1113/jphysiol.1992.sp019244.
36. **Farina D**, **Negro F.** Common synaptic input to motor neurons, motor unit synchronization, and force control. *Exerc Sport Sci Rev* 43: 23–33, 2015. doi:10.1249/JES.0000000000000032.
37. **Mannard A**, **Stein RB.** Determination of the frequency response of isometric soleus muscle in the cat using random nerve stimulation. *J Physiol* 229: 275–296, 1973. doi:10.1113/jphysiol.1973.sp010138.
38. **Negro F**, **Holobar A**, **Farina D.** Fluctuations in isometric muscle force can be described by one linear projection of low-frequency components of motor unit discharge rates. *J Physiol* 587: 5925–5938, 2009. doi:10.1113/jphysiol.2009.178509.

39. **Hug F**, **Del Vecchio A**, **Avrillon S**, **Farina D**, **Tucker KJ.** Muscles from the same muscle group do not necessarily share common drive: evidence from the human triceps surae. *J Appl Physiol (1985)*. doi:10.1152/japplphysiol.00635.2020.
40. **Negro F**, **Farina D.** Factors influencing the estimates of correlation between motor unit activities in humans. *PLoS One* 7: e44894, 2012. doi:10.1371/journal.pone.0044894.
41. **Loeb GE.** Asymmetry of hindlimb muscle activity and cutaneous reflexes after tendon transfers in kittens. *J Neurophysiol* 82: 3392–3405, 1999. doi:10.1152/jn.1999.82.6.3392.
42. **De Luca CJ**, **Gonzalez-Cueto JA**, **Bonato P**, **Adam A.** Motor unit recruitment and proprioceptive feedback decrease the common drive. *J Neurophysiol* 101: 1620–1628, 2009. doi:10.1152/jn.90245.2008.
43. **Laine CM**, **Yavuz SU**, **Farina D.** Task-related changes in sensorimotor integration influence the common synaptic input to motor neurones. *Acta Physiol* 211: 229–239, 2014. doi:10.1111/apha.12255.
44. **Doguet V**, **Jubeau M.** Reliability of H-reflex in vastus lateralis and vastus medialis muscles during passive and active isometric conditions. *Eur J Appl Physiol* 114: 2509–2519, 2014. doi:10.1007/s00421-014-2969-8.
45. **Alessandro C**, **Barroso FO**, **Prashara A**, **Tentler DP**, **Yeh HY**, **Tresch MC.** Coordination amongst quadriceps muscles suggests neural regulation of internal joint stresses, not simplification of task performance. *Proc Natl Acad Sci U S A*, 2020. 201916578. doi:10.1073/pnas.1916578117.
46. **Hug F**, **Hodges PW**, **van den Hoorn W**, **Tucker K.** Between-muscle differences in the adaptation to experimental pain. *J Appl Physiol (1985)* 117: 1132–1140, 2014. doi:10.1152/japplphysiol.00561.2014.
47. **Mellor R**, **Hodges PW.** Motor unit synchronization is reduced in anterior knee pain. *J Pain* 6: 550–558, 2005. doi:10.1016/j.jpain.2005.03.006.